RSC Advances

PAPER

View Article Online
View Journal | View Issue

Cite this: *RSC Adv.*, 2017, **7**, 45634

Dioxygen insensitive C_{70}/AuNPs hybrid system for rapid and quantitative glucose biosensing†

Piotr Piotrowski, Katarzyna Jakubow, Barbara Kowalewska and Andrzej Kaim *

Received 19th July 2017
Accepted 19th September 2017

DOI: 10.1039/c7ra07958c

rsc.li/rsc-advances

A novel hybrid system based on NAD-dependent glucose dehydrogenase immobilized on gold nanoparticles (AuNPs) covered with C_{70} fullerene has been developed for effective biosensing and quantitative detection of glucose. According to amperometric measurements, the new biosensor exhibited high sensitivity (26.1 μA mM^{-1} cm^{-2}), wide linear range (0.25–12.0 mM), and rapid characteristic response (3 s). These unique properties suggest that the prepared hybrid nanocomposite is very promising to find potential application as a dioxygen insensitive biosensor for rapid and quantitative detection of glucose.

Introduction

Biosensors allow simple and sensitive determination of glucose,[1] essential in both medical and industrial samples. Most of the glucose biosensors reported in the literature are based on glucose oxidase that is very stable, active and selective enzyme for the oxidation of glucose to gluconic acid. In the presence of dioxygen, hydrogen peroxide is produced simultaneously and its concentration is directly proportional to the glucose concentration in the sample. By the electrochemical oxidation of hydrogen peroxide the quantitative determination of glucose is possible.[2–4] One of the alternative enzymes that could be considered is glucose dehydrogenase (GDH), especially because of its insensitivity to oxygen[5,6] and ability to catalyse oxidation of glucose without formation of an undesirable intermediate product – H_2O_2. However, an important drawback of utilizing NAD-dependent dehydrogenases in biosensors and biofuel cells is the necessity of using nicotinamide cofactor (NAD^+) in the electrolyte solution.[4,7] In order to shuttle electrons from the enzymes to the electrode, NADH should be effectively regenerated at the appropriate potential. The redox couple of NAD^+/NADH has rather low redox potential (−0.56 V *vs.* SCE),[3,8] so its oxidation at a bare (without any modification) electrode occurs at high overpotential with the formation of nicotinamide dimers that foul the electrode surface.[9,10] In order to avoid this problem, various biological cofactors have been proposed and a number of electrocatalytic supports have been developed, including metal and carbon nanostructures, all intended to reduce the overpotential of NADH oxidation.[4,7]

Nanoparticles (NPs) are considered to be a favourable support for the immobilization of enzymes since they promote the enzyme kinetics in numerous ways.[11] Particularly, gold nanoparticles (AuNPs), due to their size dependent electronic properties,[12] high active surface area,[13] biocompatibility[14,15] and stability of the composite material made thereof became a promising platform for biosensors comprising enzymes, the more as the hybrid formulations preserved the original enzymatic activity.[16,17]

Moreover, the advantageous features of AuNPs can be enhanced by capping the gold surface with electroactive ligands. Numerous reports show that fullerene assemblies serve as excellent electron acceptors,[18] enhance charge separation and transport,[19,20] thus substantiating applications of C_{60} fullerene and its derivatives in glucose biosensing.[21–26] However, to the best of our knowledge, none of the reports described up today the application of C_{70} fullerene or its derivatives for this purpose, despite the fact that C_{70} reveals superior electron accepting properties, essential in electrocatalytic systems, when compared to C_{60}.[27] Thus, an enhanced synergistic effect by simultaneous usage of AuNPs, C_{70} fullerene and glucose dehydrogenase components should result in considerable higher catalytic efficiency of the new engineered biosensing device.

For this purpose, we first synthesized AuNPs covered with C_{70} fullerenethiol groups. To achieve this, *n*-octanethiol groups initially stabilizing AuNPs were successfully subjected to ligand exchange reaction against deprotected C_{70} fullerene *S*-acetyl malonate precursor. Effective decoration of gold nanoparticles with C_{70} fullerene malonate was confirmed by numerous analytical techniques. The synthesized C_{70}@AuNPs composite material was subsequently used with glucose dehydrogenase to modify glassy carbon (GC) electrodes for the construction of a glucose biosensor. Electrochemical characterization of the obtained system has proven its remarkable performance as a biosensor for quantitative detection of glucose.

Department of Chemistry, University of Warsaw, Pasteura 1, 02-093 Warsaw, Poland. E-mail: akaim@chem.uw.edu.pl

† Electronic supplementary information (ESI) available. See DOI: 10.1039/c7ra07958c

Experimental

Reagents

Toluene, *n*-hexane, tetrabutylammonium hexafluorophosphate, tetrabutylammonium cyanide (TBACN), hydrogen tetrachloroaurate(III), tetraoctylammonium bromide (TOAB), glucose dehydrogenase (GDH, EC 1.1.1.47 from Pseudomonas sp.), β-nicotinamide adenine dinucleotide hydrate (NAD^+, from yeast), β-nicotinamide adenine dinucleotide, reduced dipotassium salt (NADH), glutaraldehyde (GA), Nafion (5 wt% Nafion solution containing lower aliphatic alcohols and 15–20% water), 1-octanethiol, galactose, fructose, cellobiose, lactose, ascorbic acid (AA), uric acid (UA), dopamine and iodine were purchased from Sigma-Aldrich. 1,8-Diazabicycloundec-7-ene (DBU), and silica gel 70–230 mesh were obtained from Alfa Aesar. C_{70} fullerene was purchased from Bucky USA. Glucose, sodium sulphate, copper(II)sulphate pentahydrate, zinc sulphate heptahydrate, triethylamine, methylene chloride, dimethylformamide (DMF), ethanol and ethyl acetate were purchased from POCh (Poland). The 0.1 M phosphate buffer solution (PBS) at pH 8.0 was prepared from 0.1 M KH_2PO_4 and 0.1 M K_2HPO_4 (POCh). Toluene was dried over sodium and benzophenone. Other solvents were ACS grade and were used as received.

Characterization methods

ESI-MS spectra were recorded on a Micromass LCT ESI-TOF mass spectrometer equipped with an orthogonal electrospray ionization source. ^1H and ^{13}C NMR spectra were acquired on Varian Unity Plus 500 MHz spectrometer using $CDCl_3$ as a solvent. The infrared measurements for C_{70} fullerene derivative were performed using Shimadzu FTIR-8400S. TEM images were registered using Libra TEM and HR-TEM images were recorded on TALOS F200X apparatus on nickel grids (200 mesh) coated with carbon film. The dynamic light scattering measurements were performed using a Zetasizer Nano ZS. XPS data was collected using a VG ESCALAB 210 electron spectrometer equipped with an Al K_α source (1486.6 eV). Results were calibrated using the binding energy of Au $4f_{7/2} = 84.0$ eV as the internal standard. UV-Vis spectra were collected in quartz glass cuvette using an Evolution 60 UV-Vis Spectrophotometer from Thermo Scientific. Electrochemical experiments were performed on a CHI 760E electrochemical workstation. A three-electrode system was used with glassy carbon electrode (GC) as a working electrode, Ag/AgCl (1 M KCl) as reference electrode and a Pt wire as a counter electrode. All measurements were carried out at ambient temperature 20 ± 2 °C. To avoid possible oxygen action during the measurements, deoxygenized electrolyte solution was prepared by passing high purity grade argon gas through the solution for at least 20 min. Thermogravimetric analysis was performed under high purity nitrogen atmosphere using a TA Instruments Q50 Thermal Gravimetric Analyzer with heating rate of 5 K min^{-1}.

Synthesis

61-Ethyloxycarbonyl-61-[8-(acetylthio)octyl-1-oxycarbonyl]-1,2-methano[60]fullerene (OT-C_{70}). The desired C_{70} fullerene thioacetate was synthesized according to modified Bingel procedure (Fig. 1).[28,29] To a solution of C_{70} (168 mg, 0.2 mmol) in freshly distilled toluene (120 ml) a solution of 8-(acetylthio)octyl ethyl malonate[30] (34 mg, 0.1 mmol) in toluene (5 ml), a solution of iodine (25 mg) in toluene (10 ml) and DBU (31 μl, 0.2 mmol) were added. The obtained mixture was stirred at room temperature for 16 h under at nitrogen atmosphere. After concentration using a rotary evaporator the obtained mixture was chromatographed (silica gel 70–230 mesh, toluene/*n*-hexane 1 : 1) to yield OT-C_{70} as a blackish powder. ESI-MS, FT-IR, ^1H and ^{13}C NMR spectra for synthesized fullerene derivative are presented in ESI (Fig. S1–S4†).

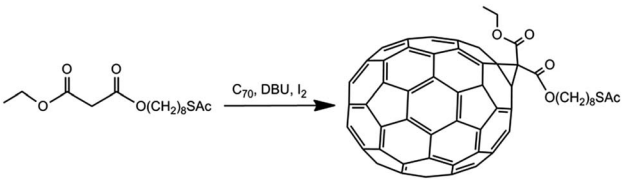

Fig. 1 Synthesis scheme for the preparation of the C_{70} thioacetate derivative (OT-C_{70}).

AuNPs ligand-exchange reaction. *n*-Octanethiol stabilized gold NPs were prepared using a modified Brust–Schiffrin procedure.[31] The use of the synthetized C_{70} fullerene derivative in its thioacetate form did not allow for grafting of functionalized fullerenes onto the AuNPs surface. For this purpose, the *S*-acetyl group was deprotected using TBACN,[32] the resulting organic layer was dried under reduced pressure and redissolved in toluene. 0.5 mM toluene solution of the deprotected ligand (5 ml) was added to diluted solution of synthesized gold NPs (200 μl in 10 ml of toluene). The obtained mixture was stirred for 72 h at room temperature under nitrogen atmosphere, without visible precipitation and/or colour changes occurring. The resulting solution was concentrated on rotary evaporator and ethanol was added to precipitate obtained nanoparticles. Obtained solution was then centrifuged, resulting precipitate was dissolved in toluene using ultrasound and again centrifuged after careful addition of ethanol, which allowed to precipitate NPs and leave traces of ligand dissolved. NPs were washed with toluene several times, till the C_{70} fullerene derivative was not detected in supernatant. The obtained nanoparticles covered with C_{70} derivative were subsequently analysed by DLS, UV-Vis, CV, XPS and TGA measurements.

Preparation of GC/OT-C_{70}@AuNPs–GDH. The glassy carbon electrode (GC, $A = 0.071$ cm^2) was successively polished with 0.5 μm and 0.05 μm alumina powders. The bioelectrocatalytic layer was prepared by dropping 5 μl of OT-C_{70}@AuNPs suspension onto the GC electrode and dried at the room temperature. Then, 7 μl from solution containing 1 mg GDH, 2 μl of 5% GA and 25 μl of PBS at pH 8.0 were placed onto the modified electrode and allowed to dry. Finally, the GC/OT-C_{70}@AuNPs–GDH was immersed in the 0.5% Nafion solution and dried at ambient temperature for 20 min. The prepared electrode was stored at 4 °C in refrigerator when not in use.

Results and discussion

Characterization of OT-C_{70} covered AuNPs

The surface morphology and size of synthesized gold nanoparticles were investigated by means of TEM microscopy. The image obtained for diluted solution of OT-C_{70}@AuNPs showed a narrow size distribution and spherical shape of nanoparticles (Fig. 2, HR-TEM see ESI, Fig. S5†). Average diameter of dispersed nanoparticles calculated using obtained results was found to be 17.3 nm.

This result is in good agreement with dynamic light scattering (DLS) measurements, which sized the bare AuNPs as 17.5 nm (see ESI, Fig. S6†). On the other hand, the sample of AuNPs coated with the functionalized C_{70} fullerene displayed an average diameter of 21.4 nm (see ESI, Fig. S7†). Taking into account the maximal dimension (length) of a single C_{70} fullerene thioacetate molecule calculated by the DFT/B3LYP/6-31g* method to be 1.8 nm for the optimized structure, the average size of the gold core after reduction of the diameter by size of the OT-C_{70} molecule can be approximated to 17.8 nm, thus similar to the value obtained for bare AuNPs. This value allowed to conclude that the performed ligand exchange reaction resulted in the formation of functionalized fullerenes monolayer on the gold nanoparticles surface. Composition of obtained monolayer and chemisorption of functionalized C_{70} fullerenes on the surface of AuNPs were confirmed by means of X-ray photoelectron spectroscopy. The XPS spectrum obtained for C_{70} functionalized gold nanoparticles revealed the presence of all expected elements: gold, carbon, sulphur, nitrogen, oxygen and bromine atoms (see ESI, Fig. S8†), thus, confirming the presence of thiolate species along with the quaternary ammonium salt on the surface of gold nanoparticles.

Further insight into the composition of OT-C_{70}@AuNPs could be provided by analysis of the S 2p region of the X-ray photoelectron spectrum (Fig. 3), which shows two contributions. The first doublet attributed to thiolate species bound to the gold surface was centred at 161.9 eV and 163.1 eV,[33] coming from the S $2p_{3/2}$ and S $2p_{1/2}$ sulphur atoms respectively. Higher photoemission peaks related to free thiols were observed at 163.6 eV for S $2p_{3/2}$ and 164.8 eV for S $2p_{1/2}$.[34] Both doublets had the expected splitting of 1.2 eV and intensity ratio of 2 : 1. No higher binding energy signals[35] were observed, implying that the obtained nanomaterial did not oxidize easily during exposition to air.

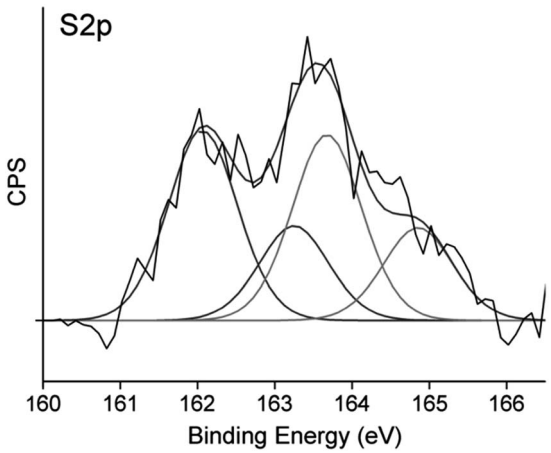

Fig. 3 XPS S 2p spectrum for OT-C_{70} deposited on gold nanoparticles surface.

Intensities of corresponding signals allowed us to determine the ratio of thiol (both octanethiol and deprotected OT-C_{70}) molecules chemisorbed using S–Au bonds and ligand molecules involved in C_{70}–Au interactions.[36] Thiol bound species contributed to 52.1% of the overall S 2p photopeak area, remaining 47.9% of sulphur atoms were attributed to the OT-C_{70} molecules bound to gold through fullerene core interactions and bearing free thiol groups. The results suggested that OT-C_{70} was the main ligand bound to AuNPs and a part of its molecules is bound to the surface of gold nanoparticles through interactions between C_{70} and Au. The possible formation of multilayer structure was excluded by DLS results which confirmed that the presence of the monolayer of OT-C_{70} molecules on the AuNPs surface. Formation of the C_{70} fullerene functionalized AuNPs was confirmed also with UV-Vis spectroscopy measurements. Absorption in the range from 300 to 700 nm was measured for 3

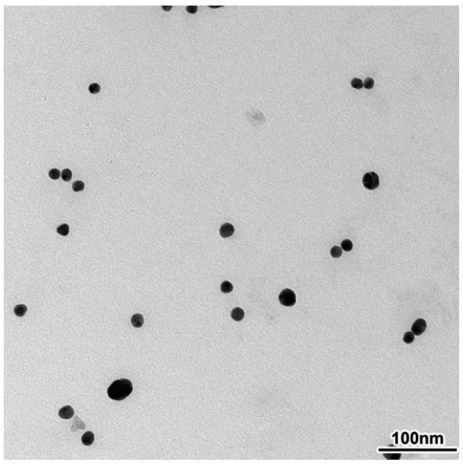

Fig. 2 TEM image of synthesized OT-C_{70}@AuNPs.

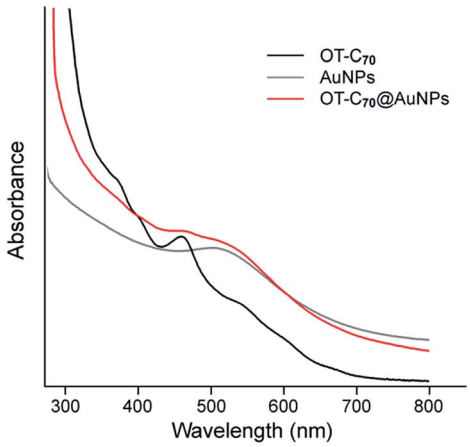

Fig. 4 UV-Vis spectra of OT-C_{70}, bare *n*-octanethiol AuNPs and OT-C_{70}@AuNPs collected from 300 to 700 nm in dichloromethane.

following samples: solution of bare *n*-octanethiol stabilized gold NPs, solution of AuNPs modified with C_{70} fullerene ligand (deprotected OT-C_{70}) and solution of OT-C_{70} in dichloromethane (Fig. 4). The C_{70} fullerene functionalized nanoparticles retained a characteristic band coming from *n*-octanethiol-AuNPs (λ_{max} = 522 nm)[37] and showed enhanced absorption attributed to the presence of C_{70} derivative, thus indicating effective ligand exchange.

The successful grafting of the functionalized C_{70} fullerene onto the gold surface, indicated by results of microscopic and spectroscopic techniques, was also confirmed by means of cyclic voltammetry. The CV curve obtained for OT-C_{70}@AuNPs showed two pair of redox peaks referring to the subsequent two one-electron quasi-reversible reductions of the C_{70} core ($\Delta E_1 = 0.254$ V and $\Delta E_2 = 0.205$ V for $C_{70}^{0/1-}$ and $C_{70}^{1-/2-}$, respectively) (Fig. 5, red line, Table S1 ESI†). The lower potential range (below −1.3 V) was not examined due to the reductive desorption of the ligand from the surface of gold observed when more negative potentials were applied.[38] Noteworthy, the observed voltammetric peaks were positively shifted comparing to the corresponding signals registered for the solution of the fullerene ligand OT-C_{70} (Fig. 5, black line, Table S1 ESI†) indicating a noticeable enhancement of the electron accepting properties due to the assembly on the surface of gold nanoparticles.

Moreover, capacitive currents were larger for the OT-C_{70}@AuNPs (red line) in comparison to the faradaic currents and the capacitance of OT-C_{70} (black line), which may be associated with an increased active surface area due to the presence of gold nanoparticles. These findings have been reported previously for AuNPs covered with C_{60} fullerene derivative.[39]

Finally, a quantitative insight into the composition of synthesized OT-C_{70}@AuNPs was given by the thermogravimetric analysis. The TGA results (Fig. 6) showed that approximately 20.5% of the total mass of the analysed nanoparticles was an organic coating: *n*-octanethiol, OT-C_{70} and TOAB, while residue after the TG analysis was recognized as a pure Au. This results imply the AuNPs surface highly covered with a heavy ligand, in this case deprotected C_{70} fullerene thioacetate.

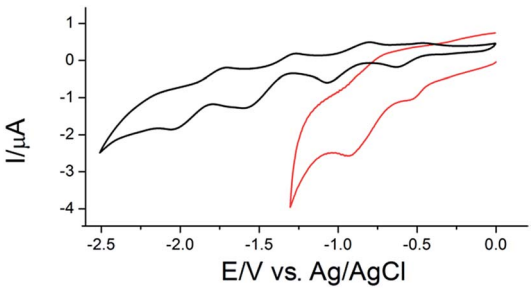

Fig. 5 Cyclic voltammograms of the C_{70} *n*-octanethiol tethered AuNPs (OT-C_{70}@AuNPs) (red line) and a pure OT-C_{70} ligand (black line) recorded in 0.1 M TBAHFP solution in toluene/acetonitrile (4 : 1), scan rate: 100 mV s^{-1}.

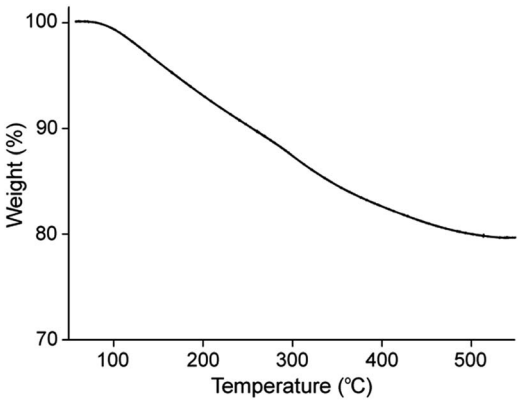

Fig. 6 Results of TG analysis obtained for the AuNPs covered with functionalized fullerenes.

Application of OT-C_{70}@AuNPs modified GC for the electrocatalytic oxidation of NADH

In this research, the cyclic voltammetry experiments were performed for the investigation of the electrocatalytic activity of OT-C_{70}@AuNPs toward the oxidation of NADH and illustrated in Fig. 7A. Upon addition of 2 mM NADH to the buffer solution, the catalytic current significantly increased at the potential *ca.* 20 mV (Fig. 7A), which can be attributed to the electrocatalytic irreversible oxidation of NADH to NAD^+ at the modified electrode. Since the oxidation of NADH at a bare GC electrode occurred at a potential of 400 mV (inset, Fig. 7A), a conclusion could be drawn that the OT-C_{70}@AuNPs lowered the overpotential by *ca.* 380 mV. These results suggest that the synthesized C_{70} fullerene derivative bond to gold nanoparticles, as the strong electron acceptor, reveal the synergistic electrocatalytic effect on the oxidation of NADH, which is likely associated with extended electroactive surface area, reduced electron-transfer resistance and unique conductive electronic structure. Simultaneously, gold nanoparticles covered with a functionalized C_{70} fullerene probably prevent the electrode fouling due to the

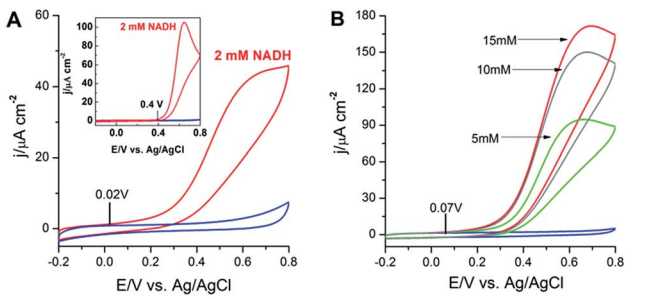

Fig. 7 (A) Voltammetric oxidation of 2 mM NADH at GC covered with OT-C_{70}@AuNPs and (inset) at bare glassy carbon electrode. Electrolyte: deoxygenated 0.1 M phosphate buffer solution at pH 8.0, scan rate: 5 mV s^{-1}. (B) Voltammetric oxidation of glucose (5, 10 and 15 mM) at GC/OT-C_{70}@AuNPs–GDH film. Electrolyte: deoxygenated 0.1 M phosphate buffer solution at pH 8.0 containing 5 mM NAD^+, scan rate: 5 mV s^{-1}. Bioelectrocatalytic oxidation and detection of glucose at the OT-C_{70}@AuNPs–GDH modified electrode.

generation of inactive dimers[9,10] and therefore, efficiently catalyse the oxidation of NADH to NAD^+ with decreasing the overpotential (in comparison to bare GC electrode) bringing closer to the thermodynamic value.

In further experiments, we diagnosed the voltammetric behaviour of the bioelectrocatalytic film with an immobilized GDH enzyme at the OT-C_{70}@AuNPs surface in the presence of the coenzyme. The substrate (glucose) and coenzyme (NAD^+) were simultaneously positioned close to the active site of the enzyme (GDH). NAD^+ is a major electron acceptor in the oxidation of glucose and the nicotinamide ring of NAD^+ accepts a hydride ion (hydrogen ion and two electrons). The reduced form (NADH) of the coenzyme generated by this reaction can be electrochemically oxidized at appropriate potential. As it is shown on cyclic voltammograms on Fig. 7B, the presence of OT-C_{70}@AuNPs and biocatalyst (GDH) had an activating effect on the glucose oxidation in neutral medium (deaerated 0.1 M phosphate buffer, pH = 8.0, containing 5 mM NAD^+). Upon the addition of 5, 10, 15 mM of glucose, the cyclic voltammograms were characterized by large anodic current densities, which corresponded to the electrooxidation of NADH produced in the enzymatic (catalysed by GDH) reaction (1):

$$\text{Glucose} + NAD^+ \rightarrow \text{gluconolactone} + \text{NADH} \quad (1)$$

The enhancement of current densities was caused by increasing glucose concentration in the buffer solution. It should be also noted that the oxidation current densities started to increase at the potential *ca.* 70 mV (close to the oxidation potential of NADH at OT-C_{70}@AuNPs without GDH enzyme). These results indicated that the electron transfer from the electrode surface to the active sites of GDH was accelerated by the OT-C_{70}@AuNPs and thus can be used as an efficient matrix for glucose biosensing.[40]

We also performed a series experiments to determine the dependence of the electrocatalytic response of the electrode on the concentration of NAD^+ coenzyme and the phosphate buffer solution pH. The maximum sensitivity was obtained for the concentration of 5 mM NAD^+ (see ESI, Fig. S9A†). The highest electrocatalytic current response was obtained at pH = 8.0 (see ESI, inset at Fig. S9A†), which is consistent with the optimum pH value for GDH dissolved in solution. The optimum pH for the enzyme activity is obviously dependent on the immobilization method and local microenvironment.

Under the optimized coenzyme concentration and pH conditions, 5 mM glucose in Ar-saturated 0.1 M PBS was diagnosed by executing comparative cyclic voltammetric measurements by the same electrode for five times. The calculated value of the relative standard deviation (RSD) of the current density (2.5%) demonstrated that the bioelectrocatalytic system is characterized by a good reproducibility. Additionally, 5 mM glucose in Ar-saturated 0.1 M PBS was measured by five modified electrodes and the RSD of the current density were 3.1% revealing an acceptable repeatability. Furthermore, the stability tests of both systems were carried out (see ESI, Fig. S9B†). When the modified electrodes were stored for 7 days in the fridge, the OT-C_{70}@AuNPs–GDH system retained 97.7% of its original response (for 15 mM glucose). After another 7 days it was 84.5%, thus it suggested that the immobilization method provides an excellent storage stability of the hybrid electrode. The slight decrease in the storage stability may be associated with the decrease of the immobilized enzyme activity or its partial leaching from the bioelectrocatalytic films during repetitive cyclic voltammetry experiments.

Fig. 8A illustrates typical chronoamperometric current–time response recorded at the film of OT-C_{70}@AuNPs and GDH enzyme (deposited on glassy carbon electrode) during successive additions of glucose. The experiment was performed under argon conditions without any redox mediator at a constant potential of 0.7 V upon the successive addition of 0.25 mM glucose. After each addition of glucose, a well-defined current increase was observed indicating very sensitive and rapid characteristic response (3 s) with a great similarity to other GDH-based biosensors, where the current increased within 1–2 s (ref. 41) or 5 s.[42] Moreover, it is better evident from the enlarged view of the part of the measurement from 0 to 500 s (inset, Fig. 8A). The calibration plot showed the steady-state current *versus* glucose concentration with the wide linearity in the range from 0.25 mM to 12 mM and detection limit 0.35 mM (inset Fig. 8B). The apparent Michaelis–Menten constant (K_M^{app}) gives an indication of the enzyme–substrate kinetics and in the present case it was calculated (from the Lineweaver–Burk plot, Fig. 8B) to be 24.1 mM. The maximum current density of the OT-C_{70}@AuNPs–GDH system was estimated to be j_{max} = 628.9 μA cm^{-2}. The obtained sensitivity value (26.1 μA mM^{-1} cm^{-2}) was much higher than those reported previously for the phenothiazine mediator system (5.1 ± 0.9 μA mM^{-1} cm^{-2}),[43] normal-length multi walled carbon nanotubes (NLMWCNT–GDH) layer (13 μA mM^{-1} cm^{-2}),[44] and MWCNT–GDH system (6.8 μA mM^{-1} cm^{-2}).[45]

To evaluate the selectivity of the OT-C_{70}@AuNPs–GDH biosensor towards glucose, other carbohydrate derivatives (such as fructose, lactose, cellobiose, and galactose), and metal ions (Zn^{2+} and Cu^{2+}) were examined (see ESI, Fig. S10†). No considerable response upon the addition of tested interfering carbohydrate molecules was observed, indicating good selectivity

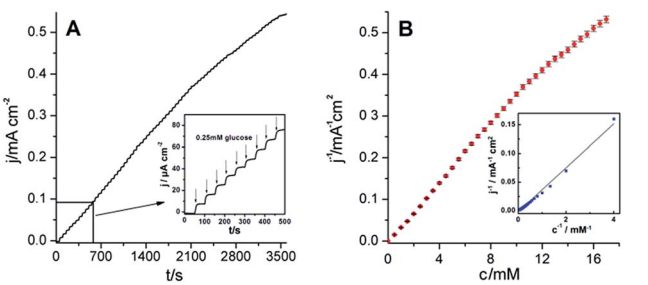

Fig. 8 (A) Amperometric response obtained at GC/OT-C_{70}@AuNPs–GDH modified electrode for successive addition of 0.25 mM glucose into Ar saturated PBS (pH 8.0) containing 5 mM NAD^+, applied potential E = 0.7 V. The inset shows enlarged view of (A). (B) The calibration curve of glucose response obtained using the data in (A) with error bars designating the standard deviation (n = 3). The Lineweaver–Burk plot is presented in inset.

toward glucose detection. Similarly, no significant current increase was detected upon the addition of ascorbic acid (AA), uric acid (UA), or dopamine (DA), suggesting that these species do not interfere with glucose detection under our experimental conditions. Thus, the effect of potential interfering compounds commonly found in biological fluids on the electrochemical detection of glucose was found to be negligible. It can be expected that the use of a thin layer of Nafion (a negatively charged polyelectrolyte) over the electrode surface can electrostatically repel the negatively charged (AA and UA) interfering compounds present in biological media.[46] Similar results were reported for other GDH/bacteria/MWCNTs[41] and GA/bacteria/GDH–bacteria/MWCNTs[42] composite films.

Conclusions

New C_{70} fullerene malonate bearing an acetyl protected thiol group was synthesized and characterized using spectroscopic techniques. After a subsequent deprotection, functionalized fullerenes were then successfully deposited onto the AuNPs surface. The DLS, UV-Vis, TGA and XPS data confirmed modification of the gold cores with C_{70} malonate, revealing that a part of OT-C_{70} molecules forming a monolayer on the AuNPs surface is bound to the gold support using strong Au–fullerene core interactions.

The proposed OT-C_{70}@AuNPs hybrid nanomaterial was shown to be a very attractive support for the immobilization of glucose dehydrogenase enzyme leading to formation of sensitive glucose biosensor. The synergistic integration of two conductive nanomaterials significantly facilitates the electron transfer between the enzyme molecule and the electrode surface improving the electrocatalytic activity toward glucose oxidation. Moreover, the application of the OT-C_{70}@AuNPs composite material causes a minimal surface fouling, while ensuring the attractive potential of NADH oxidation in neutral pH. Amperometric measurements proved the great performance (high sensitivity and reproducibility, wide linear range and low detection limit) of the prepared hybrid bioelectrocatalytic system, indicating its potential application as a dioxygen insensitive biosensor for the rapid and quantitative detection of glucose in real samples. The more so because the constructed OT-C_{70}@AuNPs–GDH biosensor was found insensitive towards potential interfering compounds usually present in biological fluids.

Conflicts of interest

There are no conflicts to declare.

Acknowledgements

Computational resources of the Interdisciplinary Centre for Mathematical and Computational Modelling at Warsaw University (Grant G15-11) were used for the theoretical sizing of optimized structure of the C_{70} fullerene thioacetate molecule. Barbara Kowalewska is thankful to the National Science Centre for the financial support under the Project SONATA UMO-2012/D7/ST5/02263.

References

1 C. Chen, Q. Xie, D. Yang, H. Xiao, Y. Fu, Y. Tan and S. Yao, *RSC Adv.*, 2013, **3**, 4473–4491.
2 B. Kowalewska and K. Jakubów, *Sens. Actuators, B*, 2017, **238**, 852–861.
3 D. Sokic-Lazic, R. L. Arechederra, B. L. Treu and S. D. Minteer, *Electroanalysis*, 2010, **22**, 757–764.
4 H. Muguruma, T. Hoshino and K. Nowaki, *ACS Appl. Mater. Interfaces*, 2015, **7**, 584–592.
5 G. Li, H. Xu, W. Huang, Y. Wang, Y. Wu and R. Parajuli, *Meas. Sci. Technol.*, 2008, **19**, 065203.
6 S. Tsujimura, S. Kojima, K. Kano, T. Ikeda, M. Sato, H. Sanada and H. Omura, *Biosci., Biotechnol., Biochem.*, 2006, **70**, 654–659.
7 B. Kowalewska and P. J. Kulesza, *Anal. Chem.*, 2012, **84**, 9564–9571.
8 F. S. Saleh, M. R. Rahman, T. Okajima, L. Mao and T. Ohsaka, *Bioelectrochemistry*, 2011, **80**, 121–127.
9 P. N. Bartlett, E. Simon and C. S. Toh, *Bioelectrochemistry*, 2002, **56**, 117–122.
10 J. Moiroux and P. J. Elving, *J. Am. Chem. Soc.*, 1980, **102**, 6533–6538.
11 V. Aggarwal and C. S. Pundir, *Methods Enzymol.*, 2016, **571**, 197–223.
12 T. A. El-Brolossy, T. Abdallah, M. B. Mohamed, S. Abdallah, K. Easawi, S. Negm and H. Talaat, *Eur. Phys. J.: Spec. Top.*, 2008, **153**, 361–364.
13 Y.-C. Yeh, B. Creran and V. M. Rotello, *Nanoscale*, 2012, **4**, 1871–1880.
14 I. Fratoddi, I. Venditti, C. Cametti and M. V. Russo, *J. Mater. Chem. B*, 2014, **2**, 4204–4220.
15 S. A. Grant, C. S. Spradling, D. N. Grant, D. B. Fox, L. Jimenez, D. A. Grant and R. J. Rone, *J. Biomed. Mater. Res., Part A*, 2014, **102**, 332–339.
16 J. M. Pingarrón, P. Yáñez-Sedeño and A. González-Cortés, *Electrochim. Acta*, 2008, **53**, 5848–5866.
17 D. Ratautas, A. Laurynenas, M. Dagys, L. Marcinkeviciene, R. Meskys and J. Kulys, *Electrochim. Acta*, 2016, **199**, 254–260.
18 E. Castro, A. Hernandez Garcia, G. Zavala and L. Echegoyen, *J. Mater. Chem. B*, 2017, **5**, 6523–6535.
19 N. Martín, L. Sánchez, B. Illescas and I. Pérez, *Chem. Rev.*, 1998, **98**, 2527–2547.
20 D. M. Guldi, B. M. Illescas, C. M. Atienza, M. Wielopolski and N. Martín, *Chem. Soc. Rev.*, 2009, **38**, 1587–1597.
21 C.-W. Chuang and J.-S. Shih, *Sens. Actuators, B.*, 2001, **81**, 1–8.
22 W. Zhilei, L. Zaijun, S. Xiulan, F. Yinjun and L. Junkang, *Biosens. Bioelectron.*, 2010, **25**, 1434–1438.
23 A. Kumar, B. Patel, G. Patel and S. K. Menon, *Fullerenes, Nanotubes, Carbon Nanostruct.*, 2010, **18**, 186–197.
24 B. Thirumalraj, S. Palanisamy, S.-M. Chen, C.-Y. Yang, P. Periakaruppan and B.-S. Lou, *RSC Adv.*, 2015, **5**, 77651–77657.

25 S. Afreen, K. Muthoosamy, S. Manickam and U. Hashim, *Biosens. Bioelectron.*, 2015, **63**, 354–364.
26 S. Pilehvar and K. De Wael, *Biosensors*, 2015, **5**, 712–735.
27 G. Diao, L. Li and Z. Zhang, *Talanta*, 1996, **43**, 1633–1637.
28 C. Bingel, *Chem. Ber.*, 1993, **126**, 1957–1959.
29 J. F. Nierengarten, V. Gramlich, F. Cardullo and F. Diedrich, *Angew. Chem., Int. Ed.*, 1996, **35**, 2101–2103.
30 P. Piotrowski, J. Pawłowska, J. G. Sadło, R. Bilewicz and A. Kaim, *J. Nanopart. Res.*, 2017, **19**, 161.
31 M. Brust, M. Walker, D. Bethell, D. J. Schiffrin and R. Whyman, *J. Chem. Soc., Chem. Commun.*, 1994, 801–802.
32 B. T. Holmes and A. W. Snow, *Tetrahedron*, 2005, **61**, 12339–12342.
33 Y. Sato, O. Niwa and F. Mizutani, *Sens. Actuators, B*, 2007, **121**, 214–218.
34 H. Hamoudi and V. A. Esaulov, *Ann. Phys.*, 2016, **528**, 242–263.
35 M. Descostes, F. Mercier, N. Thromat, C. Beaucaire and M. Gautier-Soyer, *Appl. Surf. Sci.*, 2000, **165**, 288–302.
36 N. Katsonis, A. Marchenko and D. Fichou, *Adv. Mater.*, 2004, **16**, 309–312.
37 G. Sonavane, K. Tomoda, A. Sano and K. Makino, *Colloids Surf., B*, 2008, **65**, 1–10.
38 T. W. Schneider and D. A. Buttry, *J. Am. Chem. Soc.*, 1993, **115**, 12391–12397.
39 P. Piotrowski, J. Pawłowska, J. Pawłowski, L. J. Opuchlik, R. Bilewicz and A. Kaim, *RSC Adv.*, 2014, **4**, 64310–64318.
40 P. Du, P. Wu and C. Cai, *J. Electroanal. Chem.*, 2008, **624**, 21–26.
41 B. Liang, L. Li, X. J. Tang, Q. Lang, H. Wang, F. Li, J. Shi, W. Shen, I. Palchetti, M. Mascini and A. Liu, *Biosens. Bioelectron.*, 2013, **45**, 19–24.
42 A. Liu, Q. Lang, B. Liang and J. Shi, *Biosens. Bioelectron.*, 2017, **87**, 25–30.
43 T. Hoshino, S. Sekiguchi and H. Muguruma, *Bioelectrochemistry*, 2012, **84**, 1–5.
44 H. Furutaka, K. Nemoto, Y. Inoue, H. Hidaka, H. Muguruma, H. Inoue and T. Ohsawa, *Jpn. J. Appl. Phys.*, 2016, **55**, 058001.
45 H. Zhou, Z. Zhang, P. Yu, L. Su, T. Ohsaka and L. Mao, *Langmuir*, 2010, **26**, 6028–6032.
46 H. N. Choi, M. A. Kim and W. Y. Lee, *Anal. Chim. Acta*, 2005, **537**, 179–187.